JVI Journals.ASM.org

Characterization of the Influence of Semen-Derived Enhancer of Virus Infection on the Interaction of HIV-1 with Female Reproductive Tract Tissues

Shannon A. Allen,[a] Ann M. Carias,[a] Meegan R. Anderson,[a] Eneniziaogochukwu A. Okocha,[a] Lorie Benning,[d] Michael D. McRaven,[a] Z L. Kelley,[a] John Lurain,[b] Ronald S. Veazey,[c] Thomas J. Hope[a]

Department of Cell and Molecular Biology, Feinberg School of Medicine, Northwestern University, Chicago, Illinois, USA[a]; Northwestern Memorial Hospital, Chicago, Illinois, USA[b]; Tulane National Primate Research Center, Covington, Louisiana, USA[c]; Department of Epidemiology, Bloomberg School of Public Health, Johns Hopkins University, Baltimore, Maryland, USA[d]

ABSTRACT

The majority of human immunodeficiency virus type 1 (HIV-1) transmission events occur in women when semen harboring infectious virus is deposited onto the mucosal barriers of the vaginal, ectocervical, and endocervical epithelia. Seminal factors such as semen-derived enhancer of virus infection (SEVI) fibrils were previously shown to greatly enhance the infectivity of HIV-1 in cell culture systems. However, when SEVI is intravaginally applied to living animals, there is no effect on vaginal transmission. To define how SEVI might function in the context of sexual transmission, we applied HIV-1 and SEVI to intact human and rhesus macaque reproductive tract tissues to determine how it influences virus interactions with these barriers. We show that SEVI binds HIV-1 and sequesters most virions to the luminal surface of the stratified squamous epithelium, significantly reducing the number of virions that penetrated the tissue. In the simple columnar epithelium, SEVI was no longer fibrillar in structure and was detached from virions but allowed significantly deeper epithelial virus penetration. These observations reveal that the action of SEVI in intact tissues is very different in the anatomical context of sexual transmission and begin to explain the lack of stimulation of infection observed in the highly relevant mucosal transmission model.

IMPORTANCE

The most common mode of HIV-1 transmission in women occurs via genital exposure to the semen of HIV-infected men. A productive infection requires the virus to penetrate female reproductive tract epithelial barriers to infect underlying target cells. Certain factors identified within semen, termed semen-derived enhancers of virus infection (SEVI), have been shown to significantly enhance HIV-1 infectivity in cell culture. However, when applied to the genital tracts of living female macaques, SEVI did not enhance virus transmission. Here we show that SEVI functions very differently in the context of intact mucosal tissues. SEVI decreases HIV-1 penetration of squamous epithelial barriers in humans and macaques. At the mucus-coated columnar epithelial barrier, the HIV-1/SEVI interaction is disrupted. These observations suggest that SEVI may not play a significant stimulatory role in the efficiency of male-to-female sexual transmission of HIV.

There has been great interest in the potential role that semen may play in the transmission of human immunodeficiency virus (HIV). Previous *in vitro* studies have shown that human semen enhances HIV-1 infectivity independent of tropism (1–4). Some investigations suggest a proinflammatory role when semen is introduced to the genital tract such that it alters the activation state of potential target cells and neutralizes the native acidic pH (5). Still, findings presented elsewhere suggest a target cell-specific protective effect of semen (6–9). Male-to-female HIV-1 transmission events are a consequence of exposure to semen harboring infectious virus (10). Recently, semen-derived factors that can enhance HIV-1 infectivity have received much attention. The best characterized of these factors are amyloid fibrils termed semen-derived enhancer of viral infection (SEVI), identified by fractionation of semen from healthy human donors (2, 11). SEVI is a 38-amino-acid-long fragment of the naturally occurring seminal protein prostatic acidic phosphatase (PAP), a highly expressed protein produced by the prostate organ that can persist within vaginal secretions for up to 30 h after intercourse (12). The SEVI peptide enhances infectivity only when it is in its fibrillar form and established protocols are used (2). The amount of such fibrils in semen is controversial, but a recent report demonstrated the ability to find similar structures at low levels in semen (13). In cell culture, SEVI fibrils have been shown to form complexes with HIV-1 and to facilitate virion-cell surface interactions, thereby enhancing infectivity up to 10^5-fold in cell culture at limiting viral inoculum (2). However, when tested by using the rhesus macaque transmission model, no significant enhancement of transmission mediated by either SEVI or seminal plasma (SP) was observed (14). This suggests that the cell culture systems typically used to study the potential influence of semen and SEVI on infection do

Received 9 February 2015 **Accepted** 27 February 2015

Accepted manuscript posted online 4 March 2015

Citation Allen SA, Carias AM, Anderson MR, Okocha EA, Benning L, McRaven MD, Kelley ZL, Lurain J, Veazey RS, Hope TJ. 2015. Characterization of the influence of semen-derived enhancer of virus infection on the interaction of HIV-1 with female reproductive tract tissues. J Virol 89:5569–5580. doi:10.1128/JVI.00309-15.

Editor: R. W. Doms

Address correspondence to Thomas J. Hope, thope@northwestern.edu.

doi:10.1128/JVI.00309-15

not accurately reflect the natural transmission events that occur once HIV-1 interacts with mucosal sites of infection. Better knowledge of how these seminal factors influence the interaction of HIV-1 with female reproductive tract (FRT) tissues would expand our understanding of any potential role(s) that semen plays in the sexual transmission of HIV.

The mechanism of how HIV-1 enters the epithelial barriers of intact FRT explant cultures and living macaques by percolative diffusion was recently described (15). Using a unique method to identify distinct HIV-1 particles without the encumbrance of tissue autofluorescence, we demonstrated that HIV-1 can penetrate both the vaginal and ectocervical stratified squamous and endocervical simple columnar epithelia of the lower FRT (15). For a productive infection to occur, HIV-1 must efficiently traverse these epithelia to reach target cells (16–18) located in the intra- or subepithelial compartments (15, 19). We took advantage of our ability to study the interaction of HIV-1 with mucosal sites to study the influence of SEVI on the diffusion of HIV-1 in FRT tissues.

The observed enhancing effects of SEVI are believed to be mediated by its polycationic nature. SEVI is a positively charged peptide possessing eight basic lysine and arginine residues, while cell surfaces and HIV-1 are both negatively charged (20, 21). In the context of direct infection of cells, SEVI neutralizes the repulsion between cell surfaces and HIV-1 (22). Disruption of HIV-1/SEVI interactions by mutation of lysines to neutral residues in the peptide, exposure to polyanionic molecules, or the addition of surfen results in a defect in the ability of fibrils to bind HIV-1 and potentiate infection, thus revealing the importance of electrostatic interactions (22, 23).

One major difference between mucosal tissue and a cell culture dish is the presence of mucus. Prior to virus penetration and interaction with potential target cells beneath the epithelium, semen carrying infectious virions must first interact with the cervicovaginal and endocervical mucus that blankets the FRT epithelia. Mucus is composed mostly of water (~95%) and large (megadalton) mucin proteins. Mucins contain numerous *O*-linked glycans terminating with negatively charged sialic acid molecules that contribute to the overall negative charge of mucus (24). Thus, through electrostatic mechanisms, mucus offers protection against both positively and negatively charged pathogens such as HIV. We previously demonstrated that dilution of mucus with SP enhances viral transport compared to that of mucus alone, although a similar increase in viral particle mobility was observed after dilution with phosphate-buffered saline (PBS) (25). This increase in mobility suggests that factors within semen may be beneficial to virus transport. However, the effect that semen, SP, or any seminal constituents have on virus entry into the intact FRT epithelial barriers remains unknown.

Cell culture studies clearly demonstrate that SEVI can enhance infectivity *in vitro*. However, understanding the contribution of SEVI and semen to productive male-to-female sexual transmission of HIV-1 requires the use of FRT model systems. Using our approach to label and visualize individual HIV-1 virions in tissue without the hindrance of tissue autofluorescence (15), we investigated the effects of SEVI and the semen proxy SP on HIV-1 interaction with and penetration of human explants. Furthermore, to demonstrate the importance of using *in vivo* models of transmission to validate *ex vivo* and *in vitro* studies, we also examined the effects of SEVI in the living-macaque model. We hypothesized that SEVI might bind HIV-1 to form aggregates that become sequestered on the epithelial surface, thus exhibiting inhibitory characteristics. In the current study, we reveal that independent of the presence of SEVI or SP, HIV-1 can penetrate the female genital tract epithelium similarly. The number of penetrators and their depths were influenced more by the type of tissue than by the presence of SEVI.

MATERIALS AND METHODS

HIV-1 particle generation and characterization. All virions used in this study were produced by a polyethylenimine (Polysciences) transfection method, as previously described (15, 25). For photoactivatable (PA) virions, PA-green fluorescent protein (GFP)-Vpr and proviral HIV_{R9BaL} constructs were used to cotransfect human embryonic kidney cells (HEK293T). For nonphotoactivatable virions, a GFP-Gag construct was cotransfected with a wild-type HIV_{R9BaL} proviral construct (26). After ~20 h, cells were washed with PBS and incubated in fresh media for another 16 to 24 h. Supernatants containing virus were then harvested, filtered through a 0.45-μm filter to remove cellular debris, and stored at −80°C. Prior to storage, an aliquot of each virus preparation was saved to determine the concentration titers by a p24 enzyme-linked immunosorbent assay (ELISA) (PerkinElmer). Viral stocks with a concentration of 750 ng/ml were used in tissue explant experiments. Infectivity of viral preparations was measured by using the TZM-bl indicator cell line.

SEVI preparation and functionality test. Synthetic lyophilized prostatic acidic phosphatase (PAP) protein fragment 248–286 was prepared and stained with Congo red (Sigma-Aldrich), as previously described (2). Labeled SEVI was inspected for fibril formation using fluorescence microscopy, followed by storage at 4°C. To demonstrate the ability of SEVI to interact with HIV-1 viral particles, 500 μl of 84 ng/ml R5-tropic GFP-Gag-labeled HIV_{R9BaL} was incubated with 35 μg/ml Congo red-labeled fibrils for up to 1 h at 37°C on top of coverslips in a 24-well plate. After 4 h, supernatants were aspirated, and the coverslips were fixed and mounted onto glass slides for imaging. To demonstrate the functionality of newly formed SEVI fibrils and to determine the concentration of SEVI to be used in *ex vivo* and *in vivo* experiments, 1×10^4 TZM-bl cells were sown onto a flat-bottom 96-well plate in Dulbecco's modified Eagle medium (DMEM) (Corning). Approximately 84 ng/ml HIV_{R9BaL} was incubated with 0, 5, 10, 15, 25, 50, or 100 μg/ml SEVI fibrils. Each concentration of SEVI was tested in triplicate with 100 μl of the indicated concentrations incubated previously with HIV. Virions were allowed to infect cells for 24 h before supernatants were replaced with azidothymidine (AZT) diluted with DMEM. The extent of infectivity was determined after 24 h by quantitating β-galactosidase activity. For normalization, background values determined under control conditions (no virus, SEVI only, and AZT only) were averaged and subtracted from values determined under experimental infectivity conditions.

Human SEVI explant experiments. Twelve cervical specimens were received from deidentified consenting patients undergoing either hysterectomies or cervicectomies with strict adherence to protocols approved by the Institutional Review Board at Northwestern Memorial Hospital and processed within 4 h of surgery. Cervices were separated into ectocervical and endocervical portions, followed by further dissection into 1-cm^3 cubes. Prior to the addition of tissue cubes to a 24-well plate, circular coverslips were placed into individual wells of the plate with DMEM containing 10% fetal bovine serum (FBS), 100 U/ml penicillin, 100 g/ml streptomycin, and 2 mM L-glutamine. To fully promote virus-SEVI interactions, PA-GFP-Vpr-labeled HIV_{R9BaL} (~750 ng/ml of p24) was incubated with 15 μg/ml of SEVI fibrils for up to 1 h. The lowest concentration of SEVI needed to enhance HIV-1 infectivity (15 μg/ml) was utilized, as described in the legend of Fig. 1D. Five hundred microliters of either virus alone or SEVI-bound virus was incubated with tissue pieces at 37°C. After 4 h, explants were removed from the inoculum, snap-frozen in an optimum-cutting-temperature (OCT) compound (Tissue-Tek) in standard-size plastic cryomolds (Corning), and stored at −80°C. For analysis, fro-

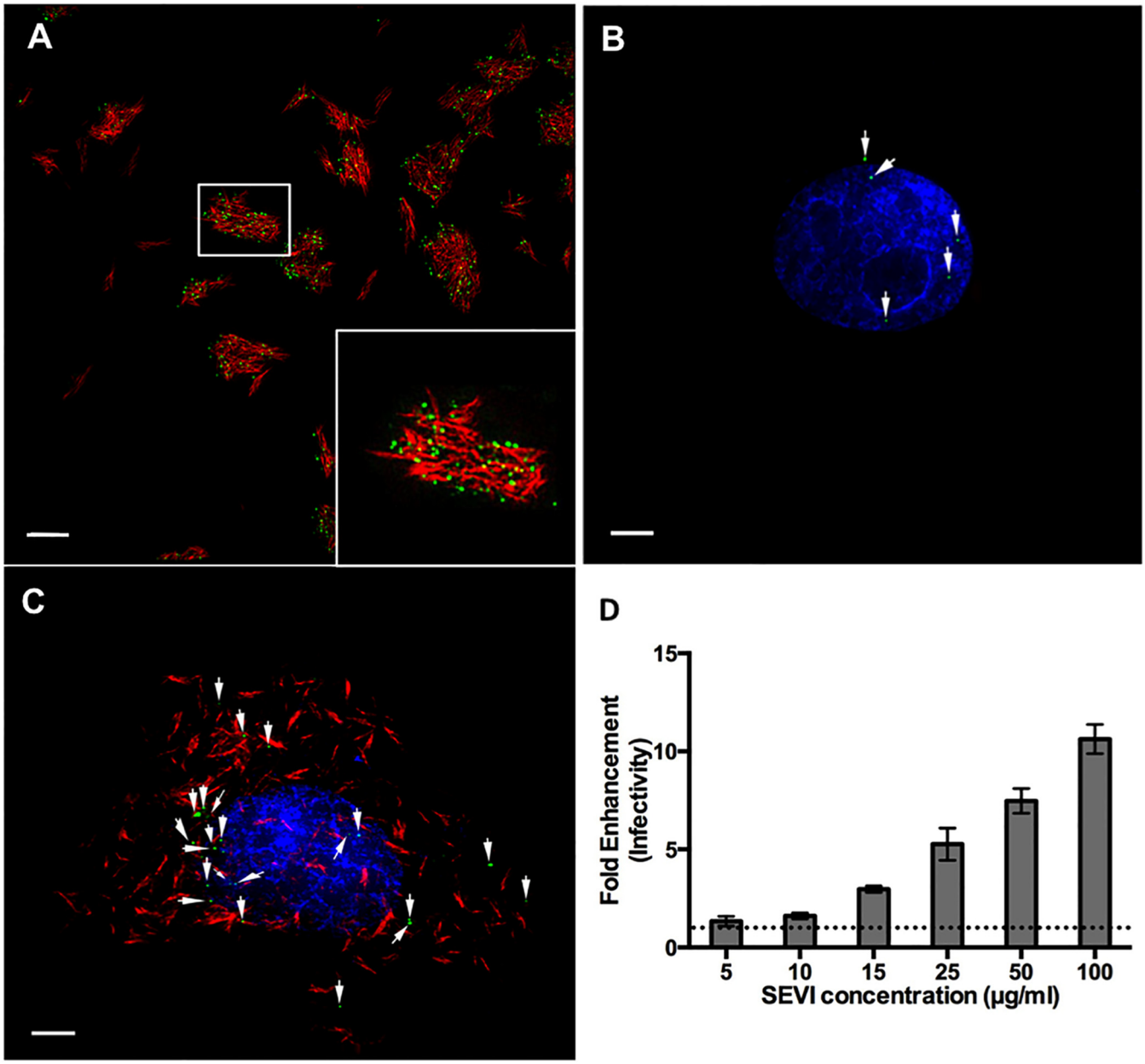

FIG 1 SEVI fibrils bind HIV-1 and enhance infection *in vitro*. (A) SEVI fibrils (red) were incubated with HIV-1 (green). (B and C) TZM-bl reporter cells, visualized by Hoechst staining (blue), were incubated with either HIV-1 alone (B) or HIV-1/SEVI complexes obtained from the assay depicted in panel A (C). (D) Effect of SEVI on HIV-1 infectivity. Data were normalized by control conditions (cells only, AZT only, and SEVI only). The dotted line represents the 0-μg/ml SEVI conditions. Fold enhancement of infectivity was obtained from 3 separate experiments performed in triplicate. Arrows in panels B and C highlight HIV-1 on cells. Images were taken at a ×100 magnification. Bars = 5 μm.

zen tissue blocks were cryosectioned at a 10-μm thickness and mounted onto slides.

Seminal plasma explant experiments. Ectocervical tissue samples were obtained following four hysterectomies. Tissue was collected, processed, and dissected into 1-cm^3 ectocervical explants. Each sample was then inoculated with 250 μl PA-GFP-Vpr-labeled HIV_{R9BaL} (~100 to 300 ng/ml of p24). To determine the effects of SP on virus entry, various dilutions of pooled SP (Lee Biosolutions) in RPMI 1640 medium (1:1, 2:1, and 3:1) were added for a 500-μl total volume. We did not demonstrate that this commercially available and widely utilized source of SP had the ability to enhance HIV infectivity in reporter assays. Samples were placed into a 5% CO_2 incubator at 37°C for 4 h and processed as described above.

Live-animal studies. All female rhesus macaques (*Macaca mulatta*) were housed at the Tulane National Primate Center, and all experiments performed were in accordance with Institutional Animal Care and Use Committee (IACUC) guidelines. Up to 1 h prior to inoculation experiments with live animals, SEVI fibrils were prepared with ~4 ml high-titer (~1,250 ng/ml p24) PA-GFP-Vpr-labeled HIV-1 viral stocks for inoculation into animals receiving SEVI. Three control animals received ~500 to ~2,000 ng/ml HIV-1, while the fourth control animal received 323 ng/μl simian-human immunodeficiency virus SF162P3. Animals were intravaginally inoculated with 4 ml of either the virus alone ($n = 4$) or the virus preexposed to SEVI ($n = 4$) for 4 h. Data from one of four control animals were collected and analyzed during this study. The data from three of the

four additional animals exposed to virus alone were acquired from a previous study done a year earlier (15). At necropsy, ectocervical, endocervical, and vaginal tissues were excised from animals, dissected into multiple pieces, and processed in the same manner as that described above for human studies.

Immunofluorescence and imaging. Sectioned tissues were fixed in a 3.7% formaldehyde–piperazine-*N*,*N*′-bis(2-ethanesulfonic acid) (PIPES) solution and blocked with normal donkey serum prior to staining. Vaginal and ectocervical tissues were stained with Cy5-conjugated wheat germ agglutinin (Invitrogen) for 30 min to define epithelial tissue structure. Endocervical explants were stained with cytokeratin 7 (DakoCytomation) for 1 h to visualize simple columnar epithelium. The nuclei of all tissues were stained with conjugated Hoechst stain (4′,6-diamidino-2-phenylindole [DAPI]) (Invitrogen) for 10 min. The secondary antibodies used during tissue experimentation included rhodamine RedX or Cy5 (Jackson ImmunoResearch). Tissue sections were then coverslipped with Dako mounting medium (DakoCytomation), sealed with nail polish, and stored at 4°C until image collection. To confirm the proper incorporation of PA-GFP into virions, p24 (AG3.0; Jonathon Allan, National Institutes of Health AIDS Research and Reference Reagent Program) and p17 (Capricorn) antibodies were used to determine the degree of colocalization with viral particles. The secondary antibodies used during *in vitro* experimentation included rhodamine RedX or Cy5.

All imaging was performed by using a 100× oil lens and a CoolSnap camera (Photometrics) mounted onto a Deltavision deconvolution microscope (Applied Precision). For all tissues, 20 to 25 images were acquired, with a total of 30 0.5-μm-thick z-stacks. Images were analyzed for the total number of virions, the number of penetrating virions, and the extent of penetration. Total virions were defined as all virions present in the entire image, including those virions observed in the lumen, stuck to the epithelial surface, and penetrating the epithelium. Penetrating virions were defined as those that entered the tissue at a distance of ≥1 μm. To determine virus penetration depths, the shortest distance from the surface of the stratified squamous or simple columnar epithelium to each virion was measured by using the Softworx distance-measuring tool (Applied Precision).

Statistical methods. Exact Wilcoxon two-sample and Kruskal-Wallis tests were used to compare the distributions of the total number of virions and the number of penetrating virions, summed across all images from each human/monkey tissue sample. To investigate differences in penetration, we first evaluated the prevalence of penetration (number of penetrating virions/total number of virions) and then evaluated the depth of penetration. Each individual virion was assigned a dichotomous indicator for penetration status, and depths were set to zero for nonpenetrating virions. Log-binomial regression models were used to assess the association between the prevalence of penetration and the presence or absence of SEVI or SP. Generalized estimating equations were used to adjust for repeated measures. *t* tests were used to compare average penetration depths per virion. *P* values of <0.05 were considered to be statistically significant. All analyses were conducted with SAS version 9 (SAS, Cary, NC, USA) or PRISM for Mac OS X (GraphPad Software). Figures were constructed by using Spotfire S+ version 8.2 (Tibco).

RESULTS

SEVI fibrils bind HIV-1 and enhance infectivity in cultured cells. Prior to characterizing the effects of SEVI on HIV-1 penetration of FRT tissues, we confirmed the functional status of the SEVI fibrils that we generated. SEVI was prepared as described previously (2, 22). Fibril formation was confirmed by successful Congo red labeling, a feature unique to amyloid proteins (Fig. 1A). We then tested whether SEVI could successfully interact with HIV-1, and similar to previous studies, labeled SEVI fibrils efficiently bound HIV-1 to form higher-order complexes (Fig. 1A) (2, 22). *In vitro* infectivity assays were then performed to define the minimum concentration of SEVI needed to enhance infectivity. Once added to cells, SEVI precipitated HIV-1 onto the cell surface and significantly enhanced HIV-1 infectivity beginning at 15 μg/ml. Enhancement of viral infectivity continued as the amount of SEVI was increased to 100 μg/ml (Fig. 1B to D). At 100 μg/ml of SEVI, HIV-1 infectivity of TZM-bl cells was increased by >10-fold. From these results, we determined that the SEVI fibrils that we generated from the synthetic SEVI peptide were functional. Based on these data, we chose a SEVI concentration of 15 μg/ml to investigate the effects of SEVI on HIV-1 penetration of FRT tissues.

SEVI reduces the frequency but not the depth of HIV-1 penetration in human ectocervix. There are two distinct types of epithelial barriers in the FRT: the vaginal vault and ectocervix are protected by a squamous epithelial barrier, while the endocervix, endometrium of the uterus, and fallopian tubes are composed of ciliated columnar epithelial cells. To evaluate the potential influence of SEVI during *ex vivo* HIV-1 exposure, we examined the interactions of HIV-1 in the presence or absence of SEVI fibrils in both endocervical (columnar epithelium) and ectocervical (squamous epithelium) explant cultures, utilizing tissues obtained from routine hysterectomies. Cervical tissues are inherently autofluorescent. Therefore, to visualize the infiltration of the FRT epithelium by individual HIV-1 virions, we used R5-tropic (BaL) photoactivatable HIV-1 (PA-HIV) to allow for efficient detection of virions (15). Comparative analysis was performed by using endocervical and ectocervical explant cultures from 12 individual donors. Twenty-five microscopic fields (512 μm by 512 μm) from both tissues from each donor in the presence and absence of SEVI were visualized. Importantly, the detection of virions after photoactivation is inherently blind, because the presence of particles cannot be determined until after a region of tissue is imaged. This aspect of the assay prevents any bias during data collection.

Using *ex vivo* and *in vivo* models of HIV-1 transmission, we previously demonstrated virus penetration of the FRT epithelium up to depths of 50 μm after 4 h of incubation with virus (15). Therefore, we visually and quantitatively assessed the influence of SEVI on the ability of PA-HIV to penetrate intact ectocervical tissue explant cultures. The total number of virions, the number and proportion of penetrating virions, and the extent of penetration were analyzed. The introduction of HIV-1/SEVI complexes into cervical tissue explant cultures could influence virion behavior and perturb the association with the epithelium, alter the penetration status, and influence the depth of virion penetration of the tissue. Therefore, we visually evaluated the influence of SEVI at the two epithelia and measured these parameters. In ectocervical tissues without SEVI treatment, PA-HIV penetrated into the stratified squamous epithelium after 4 h of inoculation (Fig. 2A), confirming previous results with this system (15). The addition of HIV-1/SEVI complexes, however, sequestered virions on the luminal surface of the stratified squamous epithelium, thus preventing these virions from entering the tissue during the 4 h of incubation in this experiment. Virions not associated with SEVI penetrated the tissue similarly to virus without treatment (Fig. 2B and Table 1).

In the ectocervix, we identified 1,876 total virions without treatment and 1,204 virions with SEVI treatment in the 300 fields examined under each condition (Table 1). Most of these virions were located at the surface of the tissue. Although there were fewer median total virions with SEVI treatment (median = 93) than with no treatment (median = 198.5), the difference was not sta-

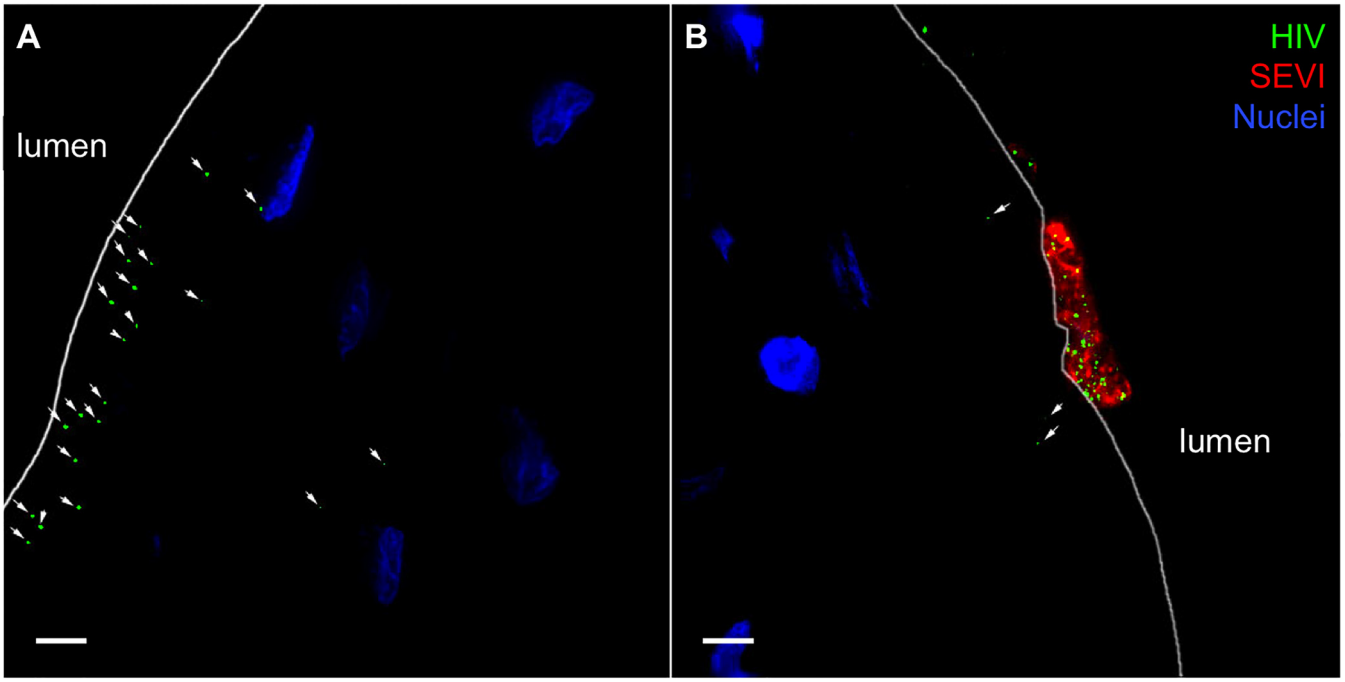

FIG 2 SEVI sequesters HIV-1 to the luminal side of human ectocervical epithelium. Labeled SEVI fibrils were incubated with PA-HIV. Either PA-HIV alone (A) or PA-HIV-1/SEVI complexes (B) were incubated with ectocervical explants. Arrows point to areas of HIV-1 ingress into the epithelium. Epithelial nuclei are identified by Hoechst staining. All images were taken at a ×100 magnification. Bars = 5 μm.

tistically significant ($P = 0.27$) (Table 1). The virions believed to be capable of causing productive infection are those that breach the FRT epithelial barrier and subsequently interact with intraepithelial and/or subbasal target cells (15, 27). Therefore, we examined the ability of SEVI to influence the penetration status of HIV. In ectocervical tissues, we identified 615 penetrating virions without treatment and 221 virions with SEVI treatment resulting in a 3-fold decrease in the frequency of observation (number of pen-

TABLE 1 Effects of SEVI treatment on the interaction of HIV with ectocervical and endocervical tissues from 12 human donors

Parameter	Value for group					
	Ectocervix			Endocervix		
	$SEVI^-$	$SEVI^+$	*P*	$SEVI^-$	$SEVI^+$	*P*
Median total no. of virions (interquartile range)[a]	198.5 (28.5, 235.5)	93 (52, 109.5)	0.26	49.5 (14, 123.5)	35.5 (8.5, 68)	0.72
Total no. of virions/total no. of images (no. of virions/image)	1,876/300 (6.25)	1,204/300 (4.01)		872/300 (2.91)	477/300 (1.59)	
Median no. of penetrators (interquartile range)[a]	56.5 (17, 80.5)	8.5 (4.5, 21)	0.02	15 (9.5, 40.5)	16.5 (7, 38)	0.98
No. of penetrators/total no. of images (no. of penetrators/image)	615/300 (2.05)	221/300 (0.737)		417/300 (1.39)	300/300 (1.00)	
No. of penetrators/total no. of virions (%)	615/1,876 (33)	221/1,204 (18)		417/872 (48)	300/477 (63)	
Prevalence ratio ($SEVI^+$ vs $SEVI^-$) (95% confidence interval)[b]	0.56 (0.34, 0.91)		0.02	1.32 (0.92, 1.89)		0.14
Avg penetration depth (μm)[c]						
Including nonpenetrators	1.55	1.05	0.001	5.65	10.08	<0.0001
Among penetrators	4.72	5.74	0.08	11.81	16.03	<0.0001
No. of penetrators <15 μm/total no. of penetrators (%)[d]	570/615 (93)	196/221 (89)	0.07	312/417 (75)	185/300 (62)	0.0002
Max penetration depth (μm)	48.7	41.5		66.7	63.1	

[a] Median numbers of virions (interquartile range) from all 12 donors. Exact Wilcoxon two-sample tests were performed to compare conditions without SEVI ($SEVI^-$) to those with SEVI ($SEVI^+$).
[b] The prevalence ratio (95% confidence interval) and *P* value were estimated from log-binomial regression models using generalized estimating equations to adjust for repeated measures.
[c] Average penetration depth per virion from all 12 donors. *t* tests were performed to compare conditions without SEVI to those with SEVI.
[d] *P* values obtained by chi-square tests.

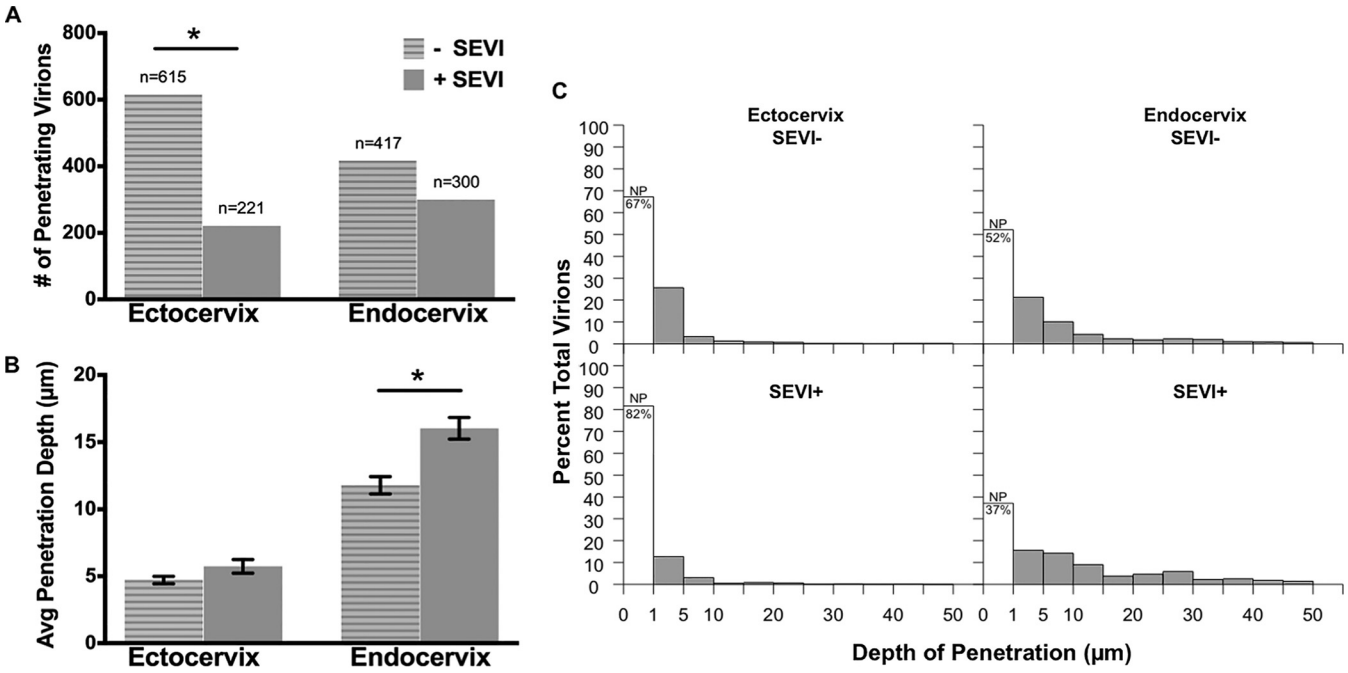

FIG 3 SEVI differentially influences the numbers and depths of penetrating virions in human cervical tissues. (A and B) Bar graphs of the number of penetrating virions (A) and average virus penetration (B) with and without SEVI treatment for ectocervix and endocervix. (C) Histograms of the distributions of penetration depths for untreated (top) and SEVI-treated (bottom) HIV-1 in the ectocervix (left) and endocervix (right). The unshaded bars within each histogram show the percentages of nonpenetrators (NP), i.e., virions that penetrated to depths of <1 μm.

etrators per image) (Fig. 3A and Table 1). The median number of penetrating virions with SEVI treatment was significantly lower than that with no treatment (8.5 versus 56.5; $P = 0.02$) (Table 1). Furthermore, the prevalence ratio of penetration (pr), or the ratio of bound virions that penetrated the tissue >1 μm, was significantly lower in the presence of SEVI (pr = 0.56; $P = 0.02$) (Table 1).

Next, we investigated whether SEVI could influence the depth of penetration of individual virions into the ectocervical epithelium. In the ectocervix, less than half of all virions under untreated (33%) and SEVI-treated (18%) conditions penetrated the epithelium (Table 1). Focusing on the virions that had penetrated the ectocervical tissue to a depth of >1 μm, we found there was no difference in the average penetration depth with (4.72 μm) and that without (5.74 μm) SEVI treatment (Fig. 3B and Table 1). To further investigate possible differences in penetration depths, we plotted the observed particle depths against the percentage of total viral particles (Fig. 3C). The distributions of particle depths with and those without SEVI were similar. Virions under both conditions penetrated the tissue in a gradient-like manner, with the majority of penetrators without SEVI (93%) and those with SEVI (89%) entering the tissue to depths of <15 μm (Table 1).

SEVI influences the depth of penetration in human endocervix but does not influence the number of HIV-1 particles entering the tissue. The same analyses were performed for endocervical tissues receiving either PA–HIV-1 alone or PA–HIV-1/SEVI complexes. In contrast to what was observed for the ectocervical explants, SEVI did not significantly alter the number of penetrating virions in endocervical explant cultures (Fig. 3A and Table 1). While there was a higher number of total and penetrating virions in the absence of SEVI treatment in the endocervix, the percentage of penetrating viral particles was higher with SEVI treatment, although this difference was not statistically significant (pr = 1.32; $P = 0.14$) (Table 1). We did observe a small (~4-μm) but statistically significantly greater average depth of virus penetration with SEVI treatment ($P < 0.0001$). However, the 4-μm increase that we observed may not be biologically significant because it is much smaller than the depth of a single columnar epithelial cell. Interestingly, virions penetrated the tissue more deeply with SEVI treatment, which has the potential to increase the ability of the virus to contact a target cell (Fig. 3B and Table 1). The observation that the virus could enter the tissue more deeply even though it was no longer associated with SEVI suggests that SEVI might be influencing the explant culture in unanticipated ways. Similarly to the ectocervix, the majority of particles entered the simple columnar epithelium in a gradient-like manner regardless of the presence of SEVI (Fig. 3C).

In endocervical explant cultures, untreated and SEVI-treated PA-HIV particles were observed on the surface of and entering the simple columnar epithelium (Fig. 4A and B). However, visualization of SEVI within the epithelium yielded unanticipated results with a loss of the original fibrillar structure. Instead, we detected a more spherical conformation of SEVI within the simple columnar epithelium (Fig. 4C). Additionally, we saw a lack of HIV-1 particles associated with SEVI while SEVI was in this spherical conformation in endocervical tissue. These data indicate that culture with endocervical epithelium disrupts the interaction between SEVI and HIV.

The fibrillar structure of SEVI is altered when introduced into human endocervical tissues. The differing effects of SEVI on virus penetration of ectocervical and endocervical tissues prompted us to investigate possible causes of these observations.

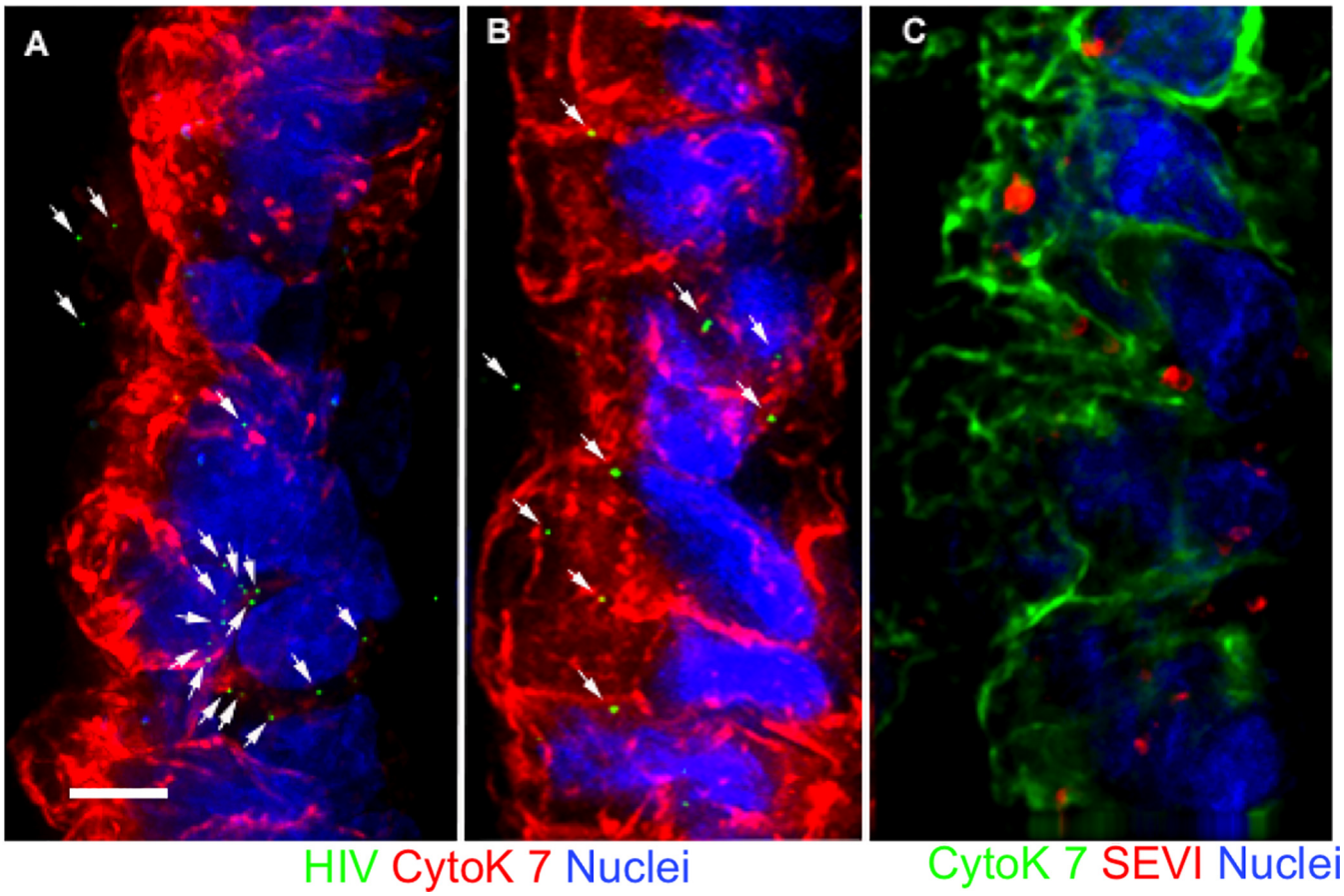

FIG 4 Untreated and SEVI-treated HIV-1 particles enter the epithelium similarly in human endocervical explants. SEVI fibrils were preincubated with PA–HIV-1. (A and B) Either PA–HIV-1 alone (A) or PA–HIV-1/SEVI complexes (B) were incubated with endocervical explants. (C) Physical appearance of SEVI within the simple columnar epithelium of the endocervix. Arrows in panels A and B highlight HIV-1 within the epithelium. The simple columnar epithelium is visualized by cytokeratin 7 staining and nuclear Hoechst staining. For each panel, the lumen is on the left side of the image. Images were taken at a ×100 magnification. Bars = 5 μm.

Therefore, we visualized the physical state of HIV-1/SEVI complexes that fell onto the coverslip placed underneath the tissue during culture (Fig. 5). In the ectocervix, PA-HIV remained bound to SEVI, forming higher-order aggregates (Fig. 5A). Of note, not all virions were bound by SEVI after incubation with ectocervical tissues. In contrast, visualization of SEVI with endocervical tissues yielded an unexpected result. A small amount of the cervical mucus produced by goblet cells within the endocervical epithelium fell onto the coverslip along with SEVI and virions. Within the mucus, SEVI was no longer fibrillar but assumed a spherical conformation. Similarly, in separate experiments, we mixed human cervical mucus with SEVI and observed a loss of fibril morphology (data not shown). Surprisingly, with this conformation, we did not observe the typical association of HIV-1 with SEVI when SEVI was in its fibrillar form (Fig. 5B). These data indicate that the aqueous environment of mucus might destabilize the fibers of SEVI.

Seminal plasma does not influence HIV-1 penetration status or depth in human ectocervical explants. As described above, the presence of preformed SEVI fibrils did not have a dramatic effect on the interaction of HIV-1 with ectocervical and endocervical explants. Because of the artificial nature of the preformed SEVI fibrils, we next examined the potential influence of SP on the interaction of HIV-1 with the human ectocervical explant cultures. In order to assess the effect of SP on virus penetration of the epithelium, we applied virus and various dilutions of SP. Overall, our data revealed no evidence of differences in the number of total virions between SP-treated and untreated tissues (Table 2). Additionally, we examined the ability of SP to influence the HIV-1 penetration status. Under untreated conditions, 22 (20%) virions penetrated the ectocervical stratified squamous epithelia, while with SP, 13 (32%), 11 (15%), 55 (42%), and 24 (18%) virions of the total viral populations were penetrators at various dilutions. There was no substantial trend in the number of penetrating virions among the various concentrations of SP (Table 2). Although the prevalence of penetration was marginally lower with SP dilutions of 2:1 (pr = 0.72; $P = 0.05$) and marginally higher with dilutions of 3:1 (pr = 1.95, $P = 0.05$) than in the untreated samples, there was no statistical difference when SP was applied at a 1:1 dilution (pr = 1.52; $P = 0.13$) or a 4:1 dilution (pr = 0.83; $P = 0.54$) (Table 2). Moreover, we found no difference in the average depth of penetration.

SEVI fibrils slightly influence the depth of HIV-1 penetration in macaque vaginal epithelium. Using the live-macaque model of transmission, previous studies detected penetrating virions within the various FRT epithelia within 4 h of virus exposure (15). We intra-

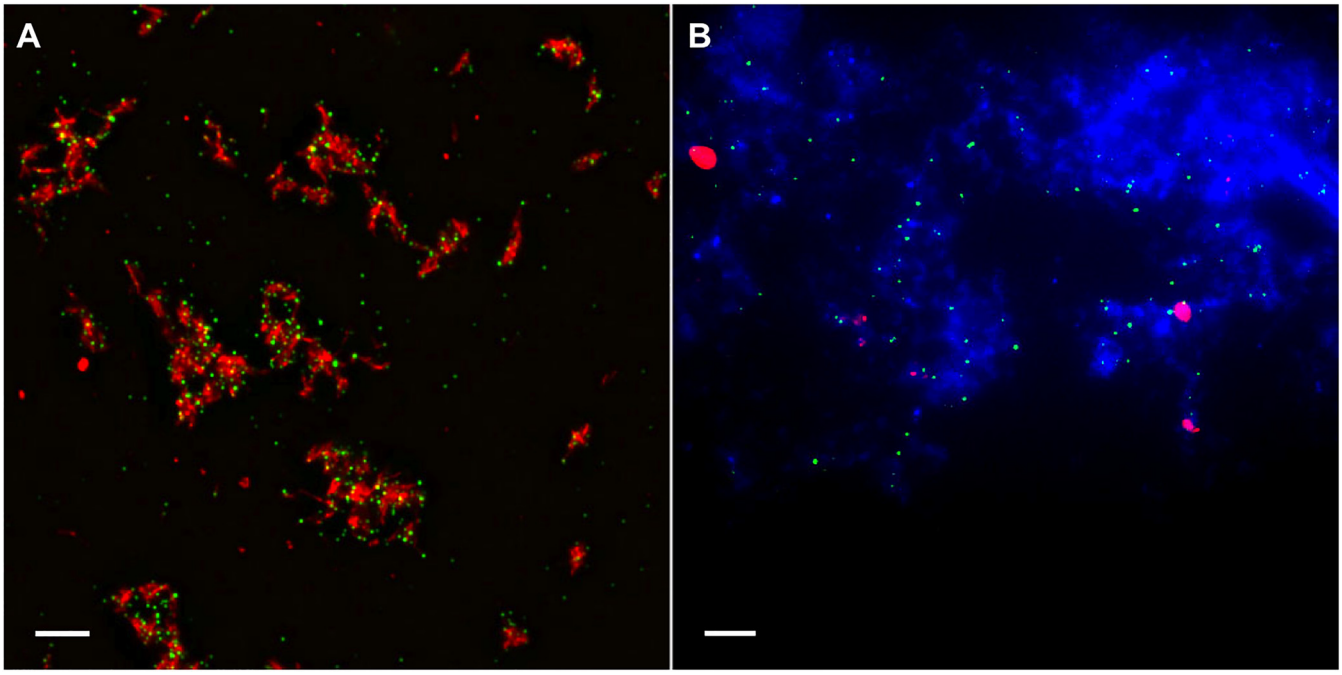

FIG 5 HIV-1 detaches from SEVI fibrils after inoculation with endocervical tissues. Shown are images of PA-HIV (green) and SEVI (red) complexes on a coverslip placed underneath ectocervical explants (A) and endocervical explants actively secreting mucus (blue) (B) during culture. Representative images from each tissue type (ectocervix and endocervix) reflect similar findings for all 12 donors. Images were taken at a ×100 magnification. Bars = 5 μm.

vaginally inoculated four female rhesus macaques with PA–HIV-1/SEVI aggregates for 4 h and compared the results to those for four previously described female rhesus macaques after exposure to PA-HIV alone (15). Similar to human tissues, the presence of SEVI led to fewer penetrating virions in ectocervical and vaginal tissues, although this decrease did not reach significance (Fig. 6A and Table 3). The only statistically significant difference was observed for the vagina, where the average depth of penetration of HIV-1 was decreased by <2 μm in the presence of SEVI. Although this difference achieved statistical significance, it is likely not biologically significant because it is such a small difference (Fig. 6B and Table 3). The distributions of depths by untreated and SEVI-treated HIV-1 in macaque ectocervix and vagina showed that the majority of virus was superficial, penetrating <1 μm, and that penetrators exhibited gradient-like penetration, with most diffusing <15 μm into the epithelium (Fig. 6C and Table 3).

TABLE 2 Effects of seminal plasma treatment on the interaction of HIV with ectocervical tissues from 4 human donors

Parameter	Value for group[e]					
		Treated with dilution of medium to SP of:				
	Untreated	1:1	2:1	3:1	4:1	*P* value
Median total no. of virions (range)[a]	25 (8–34)	14 (5–18)	19 (5–23)	15 (2–59)	25.5 (18–54)	0.26
Total no. of virions/total no. of images (no. of virions per image)	110/93 (1.18)	41/67 (0.61)	73/88 (0.83)	132/98 (1.35)	137/90 (1.52)	
No. (%) of penetrators	22 (20)	13 (32)	11 (15)	55 (42)	24 (18)	
Prevalence ratio (*P* value)[b]	NA	1.52 (0.13)	0.72 (0.05)	1.95 (0.05)	0.83 (0.54)	
Avg penetration depth (μm)[c]						
Including nonpenetrators	1.28	2.86	1.41	2.55	1.19	0.08
Among penetrators	6.39	9.03	9.35	6.11	6.80	0.65
No. of penetrators <15 μm/total no. of penetrators (%)[d]	20/22 (91)	10/13 (77)	9/11 (82)	49/55 (89)	21/24 (88)	0.71

[a] Values shown are medians (ranges [minimum to maximum]); the *P* value was determined by a Kruskal-Wallis test comparing the distributions of the total number of virions per 20 images in each of 4 donors.
[b] The prevalence ratio and *P* value were estimated from log-binomial regression models weighted by the inverse of the number of images per donor and by using generalized estimating equations to adjust for repeated measures.
[c] Average penetration depth per virion over all 4 donors. One-way analysis of variance was performed for comparisons across dilution groups.
[d] *P* value determined by a Fisher exact test.
[e] NA, not applicable.

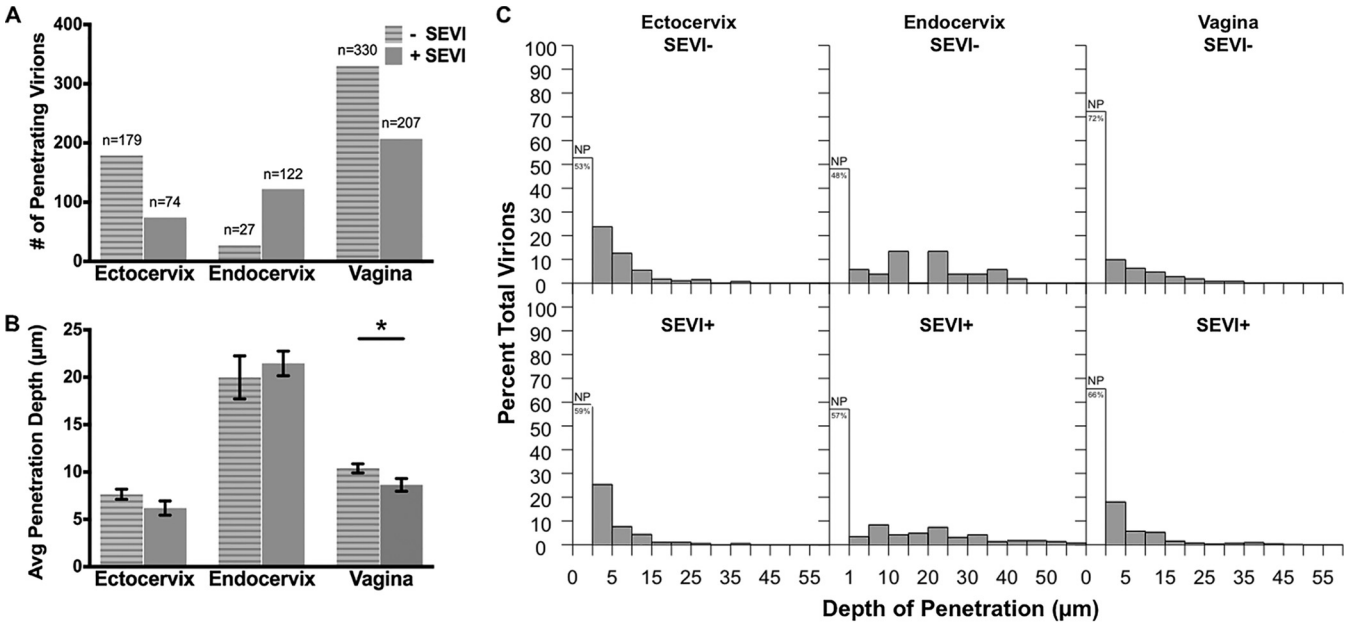

FIG 6 Virus penetration is dependent on tissue type and not SEVI in macaque genital tissues. (A and B) Bar graphs of the number of penetrating virions (A) and average virus penetration (B) with and without SEVI treatment for macaque ectocervix, endocervix, and vagina. (C) Histograms of penetration depths for untreated (top) and SEVI-treated (bottom) HIV-1 in macaque genital tissues (ectocervix [left], endocervix [middle], and vagina [right]). The unshaded bars in each panel show the percentages of nonpenetrators (NP).

In the endocervix, the number of penetrating virions was increased with SEVI treatment, and these virions, on average, exhibited deeper penetration than did untreated virions (Table 3). However, the increased number of penetrating virions and depth of penetration were found not to be statistically significant. Less than half of all virions with SEVI treatment (43%) penetrated the epithelium >1 μm, while the majority of untreated virions (52%) entered the tissue more than this distance (1 μm), although this difference was not statistically different (pr = 0.85; $P = 0.57$) (Fig. 6C and Table 3).

DISCUSSION

The knowledge that components purified from semen can stimulate HIV-1 infection up to 10^5-fold in certain cell culture systems has generated great interest toward understanding the potential role that semen might have in facilitating the sexual transmission of HIV. It is worth noting that this enhancement was observed in experiments using a limiting viral inoculum. In typical reporter cell cultures, as shown in Fig. 1, the enhancement is more typically ~10-fold (2). It is clear that SEVI and other semen-derived factors, such as semenogelin, can stimulate HIV-1 infection in many cell culture models (2, 28). However, studies to demonstrate the potential role of semen-derived factors such as SEVI in the rhesus macaque vaginal transmission model generated results that conflict with results of cell culture experiments (14). These conflicting data generated the following important question: How could conditions that lead to up to a 10^5-fold enhancement in infectivity in certain cell culture models show no effect in the highly relevant macaque vaginal challenge model? These contradictory data illustrated a large discrepancy between the influence of SEVI on HIV-1 infection of target cells *in vitro* and virus interactions with intact mucosal epithelial barriers of the FRT. To address these potential differences, we examined the interaction of individual virions with intact mucosal surfaces of human endocervical and ectocervical explants and after vaginal exposure in the rhesus macaque model in the presence and absence of SEVI fibrils or SP. We found that the presence of SEVI or SP had differential influences on the interaction of HIV-1 with the squamous epithelium and columnar epithelium of the FRT. Our data potentially explain the observed lack of an effect when SP or SEVI was present in the rhesus macaque vaginal transmission model.

We have recently reported that HIV-1 penetrates the squamous epithelium of the vaginal vault and ectocervix through the process of percolative diffusion (15). Particles of HIV-1 are small enough that they can enter the squamous epithelium through water absorption, where water-tight barriers are degraded; that is, where water can penetrate the tissue, HIV-1 can also penetrate the tissue. Both virus and water enter the tissue by moving between cells of the squamous epithelium. Here we showed that SEVI formed large complexes with multiple virions and that the presence of SEVI decreased the number of penetrating virions in the squamous epithelium of ectocervical explants by nearly 3-fold (Fig. 2B and Table 1). These data revealed that the HIV-1 particles present in these large complexes cannot fit into the small spaces between the cells and thus were trapped at the surface of the intact squamous epithelium. However, those virions not associated with SEVI fibrils appeared to enter the epithelium similarly to particles when SEVI was not present (Table 1). Despite a statistically significant decrease in the number of penetrating virions in the presence of SEVI, the depth of particles penetrating the tissue ≥1 μm was similar regardless of the presence of SEVI fibrils. With SEVI treatment, we noticed free virions within the epithelium and on coverslips placed underneath the tissue during tissue culture (Fig. 2B and 5A). The fact that not all virions were bound by SEVI fibrils suggested that unbound virions penetrated the tissue just as efficiently as untreated virions. Experiments utilizing SP did not

TABLE 3 Effects of SEVI treatment on the interaction of HIV with ectocervical, endocervical, and vaginal tissues from 8 rhesus macaques

Parameter	Value for group								
	Ectocervix			Endocervix			Vagina		
	$SEVI^-$	$SEVI^+$	*P*	$SEVI^-$	$SEVI^+$	*P*	$SEVI^-$	$SEVI^+$	*P*
Median total no. of virions (min, max)[a]	41.7 (25.4, 246.6)	28.3 (0, 141.25)	0.60	2.39 (0, 56.25)	42.1 (4, 135)	0.11	66.6 (34.4, 491.3)	33.3 (1.5, 215.5)	0.34
Total no. of virions/total no. of images (no. of virions/image)	379/455 (0.83)	181/380 (0.48)		52/477 (0.11)	284/500 (0.57)		1,190/1,059 (1.12)	602/900 (0.67)	
Median no. of penetrators (min, max)[a]	25.3 (11.6, 107.8)	12.1 (0, 56.3)	0.43	1.0 (0, 30)	9.3 (2, 135)	0.20	27.1 (14.9, 100.6)	17.4 (1.5, 58.5)	0.49
No. of penetrators/total no. of images (no. of penetrators/image)	179/455 (0.39)	74/380 (0.20)		27/477 (0.06)	122/500 (0.24)		330/1,059 (0.31)	207/900 (0.23)	
No. of penetrators/total no. of virions (%)	179/379 (47)	74/181 (41)		27/52 (52)	122/284 (43)		330/1,190 (28)	207/602 (34)	
Prevalence ratio ($SEVI^+$ vs $SEVI^-$) (95% confidence interval)[b]	0.85 (0.68, 1.07)		0.17	0.85 (0.48, 1.50)		0.57	1.30 (0.80, 2.10)		0.29
Avg penetration depth (μm)[c]									
Including nonpenetrators	3.61	2.53	0.03	10.38	9.22	0.58	2.88	2.97	0.79
Among penetrators	7.65	6.20	0.14	19.98	21.46	0.62	10.39	8.64	0.03
No. of penetrators <15 μm/total no. of penetrators (%)[d]	159/179 (89)	68/74 (92)	0.47	12/27 (44)	46/122 (38)	0.52	250/330 (76)	176/207 (85)	0.01
Max penetration depth (μm)	36.9	28.2		41.4	57.6		47.3	45.8	

[a] *P* values were determined by an exact Wilcoxon two-sample test comparing the distribution of the total number of virions or number of penetrators per 100 images for each animal.

[b] Prevalence ratios (95% confidence intervals) and *P* values were estimated from log-binomial regression models weighted by the inverse of the number of images per animal and by using generalized estimating equations to adjust for repeated measures

[c] Average penetration depth per virion over all 8 animals. *t* tests were performed to compare conditions without SEVI to those with SEVI.

[d] *P* values determined by chi-square tests.

change the interaction of HIV-1 with the squamous epithelium (Table 2). The association of HIV-1 with SEVI fibrils was shown previously to be responsible for increasing the ability of HIV-1 to associate with exposed target cells in cell culture systems through precipitation and charge masking (22). In this study, we demonstrated that the interaction of HIV-1 and SEVI functioned to prevent HIV-1 from entering the squamous epithelial tissue to potentially interact with underlying HIV-1 target cells.

In contrast to large HIV-1/SEVI complexes sequestered at the luminal surface of ectocervical explants, we saw a dramatic disruption of the HIV-1/SEVI complexes in endocervical explant cultures. Furthermore, we observed a dramatic change in the physical structure of SEVI aggregates in endocervical tissues (Fig. 4C and 5B). Rather than the fibrillar structures previously reported for SEVI and confirmed here, SEVI aggregates became spherical. Perhaps most importantly, we did not observe the typical association between HIV-1 and SEVI, even though this association was present before addition to endocervical explant cultures. A major difference between the endocervical and ectocervical explants is the presence of a thick layer of mucus associated with endocervical explants. Mucus is composed of water and highly glycosylated negatively charged sialomucin proteins whose hydrophobic domains are shielded from the primarily aqueous environment (29–31). The SEVI peptide sequence contains 14 hydrophobic residues and may behave similarly to mucin proteins when added to mucus (22). In this context, SEVI may assume a more energetically favorable conformation, thus shielding its hydrophobic residues from the mostly aqueous environment. In further support of this claim, previous studies investigating other amyloid proteins containing hydrophobic residues demonstrated that the fibrillar structure of these proteins is altered in a primarily aqueous environment (32) such as mucus.

Our *ex vivo* experiments demonstrated that in the human endocervix, HIV-1 was detached from nonfibrillar SEVI, which may be attributed to mucus (Fig. 5B). The *O*-linked glycans that coat mucins, including the most abundant secreted mucin within the endocervical canal, MUC5B, terminate with negatively charged carboxyl groups (24). It is possible that positively charged SEVI fibrils were destabilized in the unique aqueous environment of mucus, potentially influenced by the negatively charged mucins. The overall surface charge, or ζ-potential, of HIV-1 is −3 to −4 mV, and the ζ-potential for pig gastric mucin (PGM) is ~−35 mV (20, 30, 33, 34). Although we understand that PGM is not the same as human female genital mucin, it is likely to have similarities in ζ-potential due to the negatively charged glycans that coat both PGM and endocervical mucins such as MUC5B. It is feasible that SEVI may dissociate from the virus in favor of binding to mucins due to the higher negative charge. In further support of this hypothesis, it has been shown that polyanionic molecules induce the separation of HIV-1 from SEVI fibrils (22), again suggesting that SEVI favors binding to molecules that are more negatively charged than the virus. The nonfibrillar structure of SEVI was also observed within endocervical epithelial cells. Previous studies demonstrated that live epithelial cells can internalize SEVI by capturing it through extracellular protrusions (2). The highly active simple columnar epithelium of the endocervix may also possess the ability to internalize even nonfibrillar SEVI, since this form of SEVI was observed within the epithelium.

By using nonhuman primates in this study, we attempted to recapitulate the initial natural male-to-female transmission events that could promote HIV-1 acquisition. Because the fibrillar form of infection-enhancing SEVI has not been exclusively identified in semen until recently (13), we exogenously applied SEVI and virions to the genital tracts of living female rhesus macaques. The lack of any clear influence of SEVI on the interaction of HIV-1 with the mucosal barriers of rhesus macaques after vaginal exposure suggests that SEVI may not influence vaginal transmission of HIV. Supporting this view, Munch and colleagues applied SEVI or SP and simian immunodeficiency virus (SIV) to the genital tracts of live female rhesus macaques (14). After monitoring plasma viral loads, neither SEVI nor SP significantly enhanced genital mucosal transmission rates of SIV in these animals after repeated vaginal exposures (14). Those authors attributed these unexpected results to the type of virus used, the drastically weak ability of SEVI or SP to enhance SIV infectivity compared to HIV-1 *in vitro*, and the fact that macaques were nonsynchronized with regard to menstrual cycle phase. In the current macaque study, these caveats are inconsequential, since we utilized HIV-1 (not SIV), and the menstrual cycle phase of female macaques used in this study was not considered. We obtained similar results in our *in vivo* live-macaque model in that SEVI had either a marginal or no effect on HIV-1 penetration of the ectocervical, vaginal, or endocervical epithelia. Thus, this study provides mechanistic insight into the results observed during the transmission study by Munch and colleagues (14). A notable limitation of the work presented here was that a single laboratory-adapted viral isolate produced in an immortalized cell line was used. However, we previously found that the interaction of the virus with mucosal barriers of the FRT was envelope independent (15). Taken together, these studies demonstrate that although SEVI and SP can enhance HIV-1 infectivity in cell culture (14), they may not play a pivotal role in male-to-female transmission of HIV. In the context of male-to-female HIV-1 transmission, the correlates of transmission may lie within the FRT, and the sole role of semen, in general, is to deliver HIV-1 to these mucosal sites.

ACKNOWLEDGMENTS

We thank Rosemary Clark, Chisu Song, and Harry Taylor for their critical reviews of the manuscript.

This work was supported by NIH grants to Shannon A. Allen (T32AI060523) and Thomas J. Hope (P01AI082971 and R33AI094584).

REFERENCES

1. **Kim KA, Yolamanova M, Zirafi O, Roan NR, Staendker L, Forssmann WG, Burgener A, Dejucq-Rainsford N, Hahn BH, Shaw GM, Greene WC, Kirchhoff F, Munch J.** 2010. Semen-mediated enhancement of HIV infection is donor-dependent and correlates with the levels of SEVI. Retrovirology **7**:55. http://dx.doi.org/10.1186/1742-4690-7-55.
2. **Munch J, Rucker E, Standker L, Adermann K, Goffinet C, Schindler M, Wildum S, Chinnadurai R, Rajan D, Specht A, Gimenez-Gallego G, Sanchez PC, Fowler DM, Koulov A, Kelly JW, Mothes W, Grivel JC, Margolis L, Keppler OT, Forssmann WG, Kirchhoff F.** 2007. Semen-derived amyloid fibrils drastically enhance HIV infection. Cell **131**:1059–1071. http://dx.doi.org/10.1016/j.cell.2007.10.014.
3. **Bouvet JP, Gresenguet G, Belec L.** 1997. Vaginal pH neutralization by semen as a cofactor of HIV transmission. Clin Microbiol Infect **3**:19–23. http://dx.doi.org/10.1111/j.1469-0691.1997.tb00246.x.
4. **Tevi-Benissan C, Belec L, Levy M, Schneider-Fauveau V, Si Mohamed A, Hallouin MC, Matta M, Gresenguet G.** 1997. In vivo semen-associated pH neutralization of cervicovaginal secretions. Clin Diagn Lab Immunol **4**:367–374.
5. **Doncel GF, Joseph T, Thurman AR.** 2011. Role of semen in HIV-1 transmission: inhibitor or facilitator? Am J Reprod Immunol **65**:292–301. http://dx.doi.org/10.1111/j.1600-0897.2010.00931.x.

6. **Sabatte J, Ceballos A, Raiden S, Vermeulen M, Nahmod K, Maggini J, Salamone G, Salomon H, Amigorena S, Geffner J.** 2007. Human seminal plasma abrogates the capture and transmission of human immunodeficiency virus type 1 to CD4+ T cells mediated by DC-SIGN. J Virol **81:**13723–13734. http://dx.doi.org/10.1128/JVI.01079-07.
7. **Stax MJ, van Montfort T, Sprenger RR, Melchers M, Sanders RW, van Leeuwen E, Repping S, Pollakis G, Speijer D, Paxton WA.** 2009. Mucin 6 in seminal plasma binds DC-SIGN and potently blocks dendritic cell mediated transfer of HIV-1 to CD4(+) T-lymphocytes. Virology **391:**203–211. http://dx.doi.org/10.1016/j.virol.2009.06.011.
8. **Martellini JA, Cole AL, Venkataraman N, Quinn GA, Svoboda P, Gangrade BK, Pohl J, Sorensen OE, Cole AM.** 2009. Cationic polypeptides contribute to the anti-HIV-1 activity of human seminal plasma. FASEB J **23:**3609–3618. http://dx.doi.org/10.1096/fj.09-131961.
9. **Balandya E, Sheth S, Sanders K, Wieland-Alter W, Lahey T.** 2010. Semen protects CD4+ target cells from HIV infection but promotes the preferential transmission of R5 tropic HIV. J Immunol **185:**7596–7604. http://dx.doi.org/10.4049/jimmunol.1002846.
10. **UNAIDS.** 2012. Report on the global AIDS epidemic 2012. UNAIDS, Geneva, Switzerland.
11. **Usmani SM, Zirafi O, Muller JA, Sandi-Monroy NL, Yadav JK, Meier C, Weil T, Roan NR, Greene WC, Walther P, Nilsson KP, Hammarstrom P, Wetzel R, Pilcher CD, Gagsteiger F, Fandrich M, Kirchhoff F, Munch J.** 2014. Direct visualization of HIV-enhancing endogenous amyloid fibrils in human semen. Nat Commun **5:**3508. http://dx.doi.org/10.1038/ncomms4508.
12. **Collins KA, Bennett AT.** 2001. Persistence of spermatozoa and prostatic acid phosphatase in specimens from deceased individuals during varied postmortem intervals. Am J Forensic Med Pathol **22:**228–232. http://dx.doi.org/10.1097/00000433-200109000-00004.
13. **Easterhoff D, DiMaio JT, Liyanage W, Lo CW, Bae W, Doran TM, Smrcka A, Nilsson BL, Dewhurst S.** 2013. Fluorescence detection of cationic amyloid fibrils in human semen. Bioorg Med Chem Lett **23:**5199–5202. http://dx.doi.org/10.1016/j.bmcl.2013.06.097.
14. **Munch J, Sauermann U, Yolamanova M, Raue K, Stahl-Hennig C, Kirchhoff F.** 2013. Effect of semen and seminal amyloid on vaginal transmission of simian immunodeficiency virus. Retrovirology **10:**148. http://dx.doi.org/10.1186/1742-4690-10-148.
15. **Carias AM, McCoombe S, McRaven M, Anderson M, Galloway N, Vandergrift N, Fought AJ, Lurain J, Duplantis M, Veazey RS, Hope TJ.** 2013. Defining the interaction of HIV-1 with the mucosal barriers of the female reproductive tract. J Virol **87:**11388–11400. http://dx.doi.org/10.1128/JVI.01377-13.
16. **Gupta P, Collins KB, Ratner D, Watkins S, Naus GJ, Landers DV, Patterson BK.** 2002. Memory CD4(+) T cells are the earliest detectable human immunodeficiency virus type 1 (HIV-1)-infected cells in the female genital mucosal tissue during HIV-1 transmission in an organ culture system. J Virol **76:**9868–9876. http://dx.doi.org/10.1128/JVI.76.19.9868-9876.2002.
17. **Hu J, Gardner MB, Miller CJ.** 2000. Simian immunodeficiency virus rapidly penetrates the cervicovaginal mucosa after intravaginal inoculation and infects intraepithelial dendritic cells. J Virol **74:**6087–6095. http://dx.doi.org/10.1128/JVI.74.13.6087-6095.2000.
18. **Kaizu M, Weiler AM, Weisgrau KL, Vielhuber KA, May G, Piaskowski SM, Furlott J, Maness NJ, Friedrich TC, Loffredo JT, Usborne A, Rakasz EG.** 2006. Repeated intravaginal inoculation with cell-associated simian immunodeficiency virus results in persistent infection of nonhuman primates. J Infect Dis **194:**912–916. http://dx.doi.org/10.1086/507308.
19. **Stieh DJ, Maric D, Kelley ZL, Anderson MR, Hattaway HZ, Beilfuss BA, Rothwangl KB, Veazey RS, Hope TJ.** 2014. Vaginal challenge with an SIV-based dual reporter system reveals that infection can occur throughout the upper and lower female reproductive tract. PLoS Pathog **10:**e1004440. http://dx.doi.org/10.1371/journal.ppat.1004440.
20. **Arjmandi N, Van Roy W, Lagae L, Borghs G.** 2012. Measuring the electric charge and zeta potential of nanometer-sized objects using pyramidal-shaped nanopores. Anal Chem **84:**8490–8496. http://dx.doi.org/10.1021/ac300705z.
21. **Bondar OV, Saifullina DV, Shakhmaeva II, Mavlyutova II, Abdullin TI.** 2012. Monitoring of the zeta potential of human cells upon reduction in their viability and interaction with polymers. Acta Naturae **4:**78–81.
22. **Roan NR, Munch J, Arhel N, Mothes W, Neidleman J, Kobayashi A, Smith-McCune K, Kirchhoff F, Greene WC.** 2009. The cationic properties of SEVI underlie its ability to enhance human immunodeficiency virus infection. J Virol **83:**73–80. http://dx.doi.org/10.1128/JVI.01366-08.
23. **Roan NR, Sowinski S, Munch J, Kirchhoff F, Greene WC.** 2010. Aminoquinoline surfen inhibits the action of SEVI (semen-derived enhancer of viral infection). J Biol Chem **285:**1861–1869. http://dx.doi.org/10.1074/jbc.M109.066167.
24. **Cone RA.** 2009. Barrier properties of mucus. Adv Drug Deliv Rev **61:**75–85. http://dx.doi.org/10.1016/j.addr.2008.09.008.
25. **Shukair SA, Allen SA, Cianci GC, Stieh DJ, Anderson MR, Baig SM, Gioia CJ, Spongberg EJ, Kauffman SM, McRaven MD, Lakougna HY, Hammond C, Kiser PF, Hope TJ.** 2013. Human cervicovaginal mucus contains an activity that hinders HIV-1 movement. Mucosal Immunol **6:**427–434. http://dx.doi.org/10.1038/mi.2012.87.
26. **Leblanc JJ, Perez O, Hope TJ.** 2008. Probing the structural states of human immunodeficiency virus type 1 pr55gag by using monoclonal antibodies. J Virol **82:**2570–2574. http://dx.doi.org/10.1128/JVI.01717-07.
27. **Poonia B, Wang X, Veazey RS.** 2006. Distribution of simian immunodeficiency virus target cells in vaginal tissues of normal rhesus macaques: implications for virus transmission. J Reprod Immunol **72:**74–84. http://dx.doi.org/10.1016/j.jri.2006.02.004.
28. **French KC, Roan NR, Makhatadze GI.** 2014. Structural characterization of semen coagulum-derived SEM1(86-107) amyloid fibrils that enhance HIV-1 infection. Biochemistry **53:**3267–3277. http://dx.doi.org/10.1021/bi500427r.
29. **Bansil R, Turner BS.** 2006. Mucin structure, aggregation, physiological functions and biomedical applications. Curr Opin Colloid Interface Sci **11:**164–170. http://dx.doi.org/10.1016/j.cocis.2005.11.001.
30. **Lee S, Muller M, Rezwan K, Spencer ND.** 2005. Porcine gastric mucin (PGM) at the water/poly(dimethylsiloxane) (PDMS) interface: influence of pH and ionic strength on its conformation, adsorption, and aqueous lubrication properties. Langmuir **21:**8344–8353. http://dx.doi.org/10.1021/la050779w.
31. **Carlstedt I, Lindgren H, Sheehan JK, Ulmsten U, Wingerup L.** 1983. Isolation and characterization of human cervical-mucus glycoproteins. Biochem J **211:**13–22.
32. **Zhang S, Iwata K, Lachenmann MJ, Peng JW, Li S, Stimson ER, Lu Y, Felix AM, Maggio JE, Lee JP.** 2000. The Alzheimer's peptide a beta adopts a collapsed coil structure in water. J Struct Biol **130:**130–141. http://dx.doi.org/10.1006/jsbi.2000.4288.
33. **Mazoniene E, Joceviciute S, Kazlauske J, Niemeyer B, Liesiene J.** 2011. Interaction of cellulose-based cationic polyelectrolytes with mucin. Colloids Surf B Biointerfaces **83:**160–164. http://dx.doi.org/10.1016/j.colsurfb.2010.11.022.
34. **McGill SL, Smyth HD.** 2010. Disruption of the mucus barrier by topically applied exogenous particles. Mol Pharm **7:**2280–2288. http://dx.doi.org/10.1021/mp100242r.